



Thermo-Mechanical Characterization and Combustion Analysis of HTPB/Paraffin Wax blended Hybrid Rocket

Sasi Kiran Palateerdham, Daniele Tortorici, Antonella Ingenito³

Abstract

This study investigates the performance of hybrid rocket engines using hydroxyl-terminated polybutadiene (HTPB), paraffin wax, and their blends at varying proportions, with gaseous oxygen as the oxidizer. Thermo-mechanical characterization of the fuels was conducted to support the combustion analysis. Thermal gravimetric analysis (TGA) was used to examine the thermal decomposition behavior of the samples and to identify characteristic decomposition temperatures, while tensile testing determined key mechanical properties, including tensile strength, Young's modulus, and elongation at break, providing insight into structural integrity under operational conditions. Ballistic performance tests were carried out to evaluate the combustion behavior of the fuels, focusing on regression rate, chamber pressure, thrust, and combustion efficiency. The performance of the blended fuels was compared with that of neat HTPB and paraffin, enabling assessment of the effect of blending on both combustion characteristics and material behavior. The results indicate that HTPB–paraffin blends have the potential to enhance hybrid rocket performance and contribute to the development of optimized fuel formulations for advanced hybrid propulsion systems.

Keywords

HTPB-paraffin, Hybrid Rocket, fuel characterization, Ballistic Performance, Regression Rate, Gaseous oxidizer

1. Introduction

Hybrid rocket engines are increasingly gaining attention for aerospace launch systems and space missions due to their simple design, ease of operation, safety, and controllability. They are particularly promising for small and micro-satellite launch applications [1, 2]. Traditionally used fuels such as hydroxyl-terminated polybutadiene (HTPB) and polymethyl methacrylate (PMMA) have been widely adopted for their excellent thermo-mechanical properties. However, their relatively low regression rates and limited combustion efficiency restrict their current applications [3, 4].

In contrast, paraffin wax has emerged as a promising solid fuel for hybrid rockets due to its high regression rate, which is typically 3–4 times greater than that of conventional polymeric fuels [5]. This enhanced regression behavior arises from its unique combustion mechanism, where the formation of an unstable melt layer on the grain surface leads to droplet entrainment into the gas-phase flow field [6]. However, the practical application of paraffin is limited by its poor mechanical properties—such as high brittleness, low strength, and a tendency to crack under thermal stress—which compromise the structural integrity of fuel grains during manufacturing, handling, and motor operation [7].

Several studies have proposed blending paraffin with reinforcing binders such as ethylene vinyl acetate (EVA), polyethylene (PE), polypropylene (PP), polyurethane foam (PUF), and HTPB to address the complementary limitations of paraffin[8, 9]. Sinha et al.[10] studied the addition of HTPB into paraffin wax

¹Sapienza University of Rome, sasikiran.palateerdham@uniroma1.it

²Sapienza University of Rome, daniele.tortorici@@uniroma1.it

³Sapienza University of Rome, antonella.ingenito@uniroma1.it

to enhance the thermal stability and mechanical performance of solid fuel. Blending paraffin with HTPB has emerged as a promising strategy. Such blends combine the high regression rate of paraffin with the mechanical robustness of HTPB, resulting in improved fuel performance and grain stability [11, 12]. For instance, 50/50 paraffin—HTPB mixtures have been tested with nitrous oxide and gaseous oxygen, showing favorable regression characteristics and comparable combustion efficiency across different oxidizers [11].

Ballistic testing is essential for evaluating these hybrid fuels, as it provides insight into thrust generation, regression behavior, combustion efficiency, and thermal response under realistic operating conditions. Results consistently demonstrate that paraffin/HTPB blends achieve higher regression rates than pure HTPB while maintaining greater structural integrity than pure paraffin. Such findings highlight the importance of ballistic testing in assessing the performance potential of these blends and guiding the optimization of grain formulations for future hybrid rocket applications.

2. Materials and methods

The materials employed in this study are paraffin and hydroxyl-terminated polybutadiene (HTPB). The HTPB was synthesized using poly bd® R45 V resin as the base polymer, with dioctyl adipate (DOA) serving as a plasticizer to enhance flexibility. Toluene diisocyanate (TDI) was used as the curing agent, and glycerol was included in the formulation. We explored a series of formulations composed of paraffin—HTPB blends with varying proportions. These blends were classified according to their paraffin content, ranging from pure paraffin (100P) to pure HTPB (0P), with intermediate compositions including 70P, 50P, 35P, and 25P, as given in Table 1. This systematic variation enables a comparative analysis of how paraffin and HTPB concentration influences the physical and chemical properties of the resulting material systems.

Sample	Paraffin Wax [Wt.%]	(HTPB + DOA + TDI + Glycerol) [Wt.%]
100P	100	0
70P	70	30
50P	50	50
35P	35	65
25P	25	75
0P	0	100

Table 1. Tested HTPB–paraffin based fuel composition.

2.1. Thermo-Mechanical characterization

To evaluate the combustion-relevant and structural properties of the fuel samples, a comprehensive thermo-mechanical analysis was carried out, encompassing both thermal gravimetric analysis (TGA), differential scanning calorimetry (DSC) tests, and mechanical tensile testing. TGA and DSC measurements were performed using a TGA/DSC 3+ analyzer (METTLER TOLEDO, Greifensee, Switzerland), enabling precise characterization of the thermal decomposition behavior. Tensile tests were conducted with a 10 kN AGS-X series universal testing machine (Shimadzu Corporation, Kyoto, Japan) to determine the mechanical performance of the samples under uniaxial stress. Detailed procedures and parameters for each technique are described in the following. Each test was performed in triplicate to ensure reproducibility and enable statistical analysis.

2.1.1. Thermal analysis

Thermal gravimetric analysis and differential scanning calorimetry (TGA/DSC) were performed under a controlled nitrogen atmosphere with a constant flow of 60 mL/min. Approximately 20 mg of each fuel sample was heated from room temperature to 600 °C at a constant heating rate of 10 °C/min. The mass loss and heat flow were continuously recorded as functions of temperature in order to evaluate the thermal decomposition behavior of the fuels. The resulting thermograms were analyzed to identify

characteristic decomposition stages and corresponding onset temperatures. The melting temperature of each fuel composition, where present, was determined from the endothermic peak observed in the thermal profile together with the associated heat flow. The principal decomposition temperature was identified from the exothermic peak in the DSC curve.

2.1.2. Mechanical testing

Tensile testing of the fuel samples was carried out on standardized specimens prepared in accordance with ASTM D638. The experiments were conducted at ambient temperature using a crosshead speed of 5 mm/min for the 100P, 70P, 50P, 35P, and 25P formulations, while a higher crosshead speed of 10 mm/min was employed for the pure HTPB specimens. The resulting stress—strain curves were analyzed to extract the key mechanical parameters, including tensile strength, Young's modulus, and elongation at break.

2.2. Ballistic characterization

To further evaluate the performance of the solid fuels, a series of ballistic tests was conducted using gaseous oxygen as the oxidizer in a lab-scale static hybrid rocket motor. The test setup included a laboratory-scale motor mounted on a thrust stand, an oxidizer feed system, a pyrogen igniter, and a data acquisition system. A schematic of the experimental configuration is shown in Figure (1). The oxidizer was introduced into the combustion chamber through a stainless-steel axial flow injector. Ignition was initiated by a pyrogen igniter positioned at the head end of the motor, generating sufficient heat to exceed the ignition temperature of the fuel grain. This preheats the chamber, enabling the fuel to vaporize and react efficiently with the incoming oxygen.

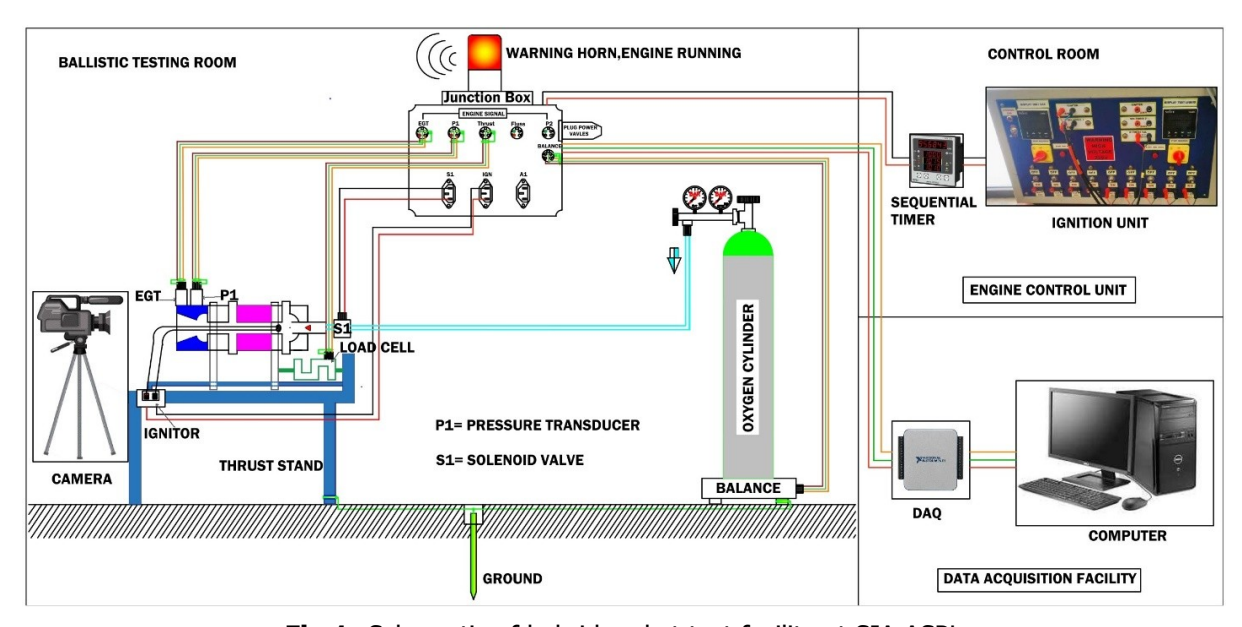


Fig 1. Schematic of hybrid rocket test facility at SIA ASPL

The combustion chamber was designed with a length of 240 mm and an inner diameter of 80 mm to accommodate the solid fuel grain. A convergent-divergent nozzle was employed, featuring a 12 mm throat diameter, a semi-convergent angle of 45° , and a semi-divergent angle of 13° . The oxidizer flow rate was regulated by a pressure regulator in combination with a solenoid valve. Each test was carried out with a burn duration of 5 seconds. Following each firing, the residual fuel grain could be easily removed from the chamber using cardboard tubes, allowing for precise post-test evaluation. This facilitated accurate measurement of the fuel regression rate and total mass consumption.

The weight loss technique is one of the most reliable and convenient methods for measuring the regression rate in hybrid rocket engines. It has been widely adopted by researchers for this purpose [13].

This approach involves determining the regression rate by measuring the initial and final masses of the solid fuel grain. In the present study, the weight loss method is used to calculate the fuel regression rate. After conducting the ballistic test, the engine is allowed to cool for at least 30 minutes. The nozzle is then dismantled, and the solid fuel grain is carefully removed. The final mass of the fuel is measured, and the difference between the initial mass (before the burn) and the final mass (after the burn) provides the total mass loss during the fire test. Dividing this net mass loss by the burn time yields the fuel mass consumption rate. The regression rate of the engine is subsequently determined as described in Eq.(1).

$$\dot{r} = \frac{d_b - d_{ig}}{2t_b} \tag{1}$$

Where d_b and d_{ig} are the fuel port diameters after burnout and before the ignition process, respectively. The burn time t_b is the time duration of the combustion, i.e., the start of ignition to the end of the oxidiser supply. The fuel port diameter after burnout can be given as in Eq.(2).

$$d_b = \sqrt{d_{ig}^2 + \frac{m_b}{\frac{\pi}{4}\rho_f l_f}} \tag{2}$$

Where m_b is the mass of burnt fuel and ρ_f is the actual measured density of the fuel, and l_f is the length of the fuel grain. The corresponding oxidiser mass flux rate can be given by Eq.(3).

$$G_{ox} = \frac{\dot{m}_{ox}}{A_p} \tag{3}$$

Where \dot{m}_{ox} is the oxidiser mass flow rate and A_p is the port combustion cross-section area, which can be calculated as given in Eq.(4).

$$A_p = \frac{\pi}{4} \left(\frac{d_b + d_{ig}}{2} \right)^2 \tag{4}$$

3. Results and discussion

3.1. Mechanical performance

Tensile testing confirmed that all fuel samples exhibit sufficient mechanical integrity for safe handling and processing. The stress–strain curves (Fig. 2) revealed notable differences in stiffness and ductility across the various formulations. Ultimate tensile strength values ranged from 108.48 ± 14.05 kPa for the pure HTPB (0P) samples to 1166.51 ± 307.27 kPa for the pure paraffin (100P) samples, with blended compositions displaying intermediate values, as detailed in Table 2. Elongation at break varied significantly: the 0P samples demonstrated high ductility with elongation exceeding 300%, whereas the 100P samples showed minimal elongation, on the order of 1%. A pronounced shift in mechanical behavior was observed between the 35P and 25P formulations, suggesting the presence of a critical composition threshold in this range where the material transitions from paraffin-dominated to HTPB-dominated characteristics.

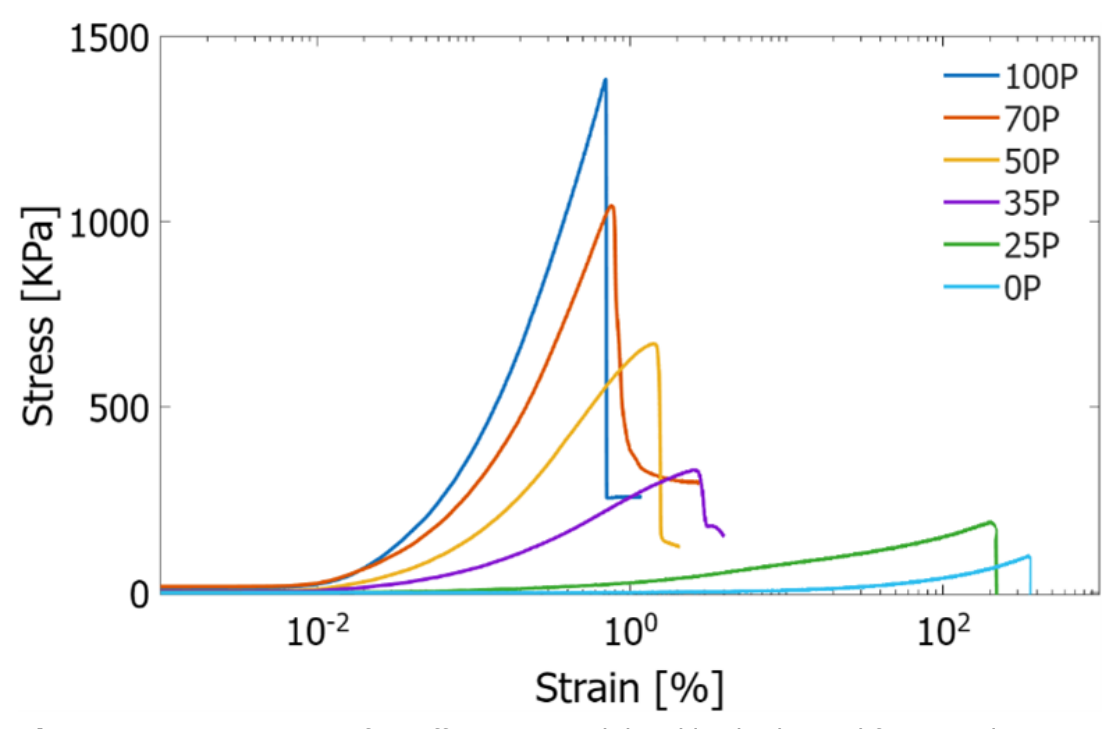


Fig 2. Stress-strain curves of paraffin, HTPB, and their blends obtained from tensile testing

Composition	Young's Modulus [MPa]	Ultimate Strength [kPa]	Elongation at Break [%]
100P	378.85 ± 9.03	1166.51 ± 307.27	0.6 ± 0.1
70P	271.72 ± 10.52	1006.49 ± 102.43	0.8 ± 0.1
50P	154.53 ± 7.68	686.17 ± 59.33	1.6 ± 0.3
35P	57.91 ± 11.99	340.02 ± 19.16	2.1 ± 0.3
25P	1.00 ± 0.30	187.85 ± 8.43	167 ± 36.3
0P	0.05 ± 0.01	108.48 ± 14.05	365 ± 17.7

Table 2. Tensile test results for paraffin/HTPB fuel samples at varying composition.

3.2. Thermal characterization

Thermogravimetric analysis (TGA, Fig. 3) revealed distinct decomposition profiles across all fuel compositions. The 100P and 0P samples, representing the two unblended formulations—pure paraffin and pure HTPB, respectively— exhibited onset decomposition temperatures of 312.4 ± 7.1 °C and 416.0 ± 2.5 °C. These results indicate a significantly higher thermal stability for HTPB compared to paraffin, suggesting that blended formulations should exhibit intermediate thermal behavior. This trend is confirmed by the onset temperatures of the blended samples (70P, 50P, 35P, and 25P), as summarized in Table 3.

Complementary thermal data, shown in Fig. 4, were obtained via differential scanning calorimetry (DSC) curves, offering deeper insight into the thermal transitions. Endothermic peaks associated with melting were observed in paraffin-containing samples, with melting temperatures ranging from 65.5 ± 0.1 °C for the 100P formulation to 63.2 ± 0.4 °C for the 25P formulation. In contrast, the 0P sample exhibited no detectable melting transition, indicating that HTPB undergoes degradation without melting. The decomposition temperature, identified by the peak of exothermic events, ranges from 402.1 ± 9.8 °C for the 100P samples to 368.1 ± 2.3 °C for the pure HTPB samples. While the endothermic activity tends to diminish with increasing HTPB content, the exothermic response near the decomposition peak becomes progressively more pronounced as the HTPB concentration rises. Table 4 presents data corresponding

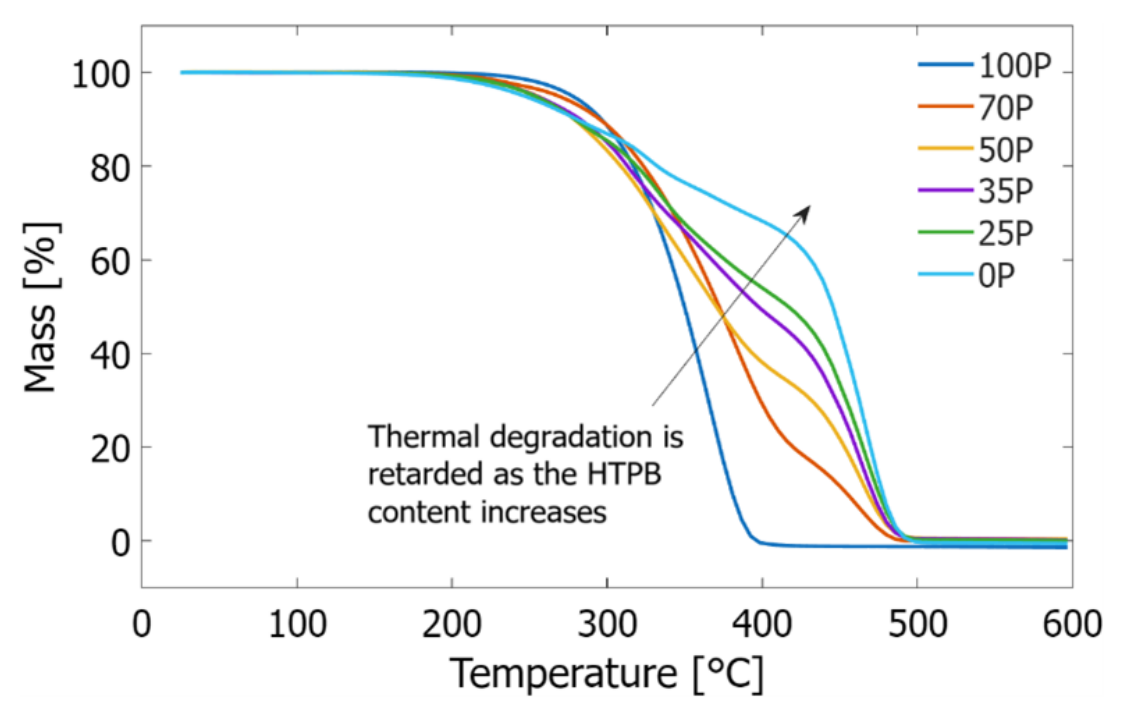


Fig 3. TGA curves showing the thermal decomposition behavior of paraffin, HTPB, and their blends

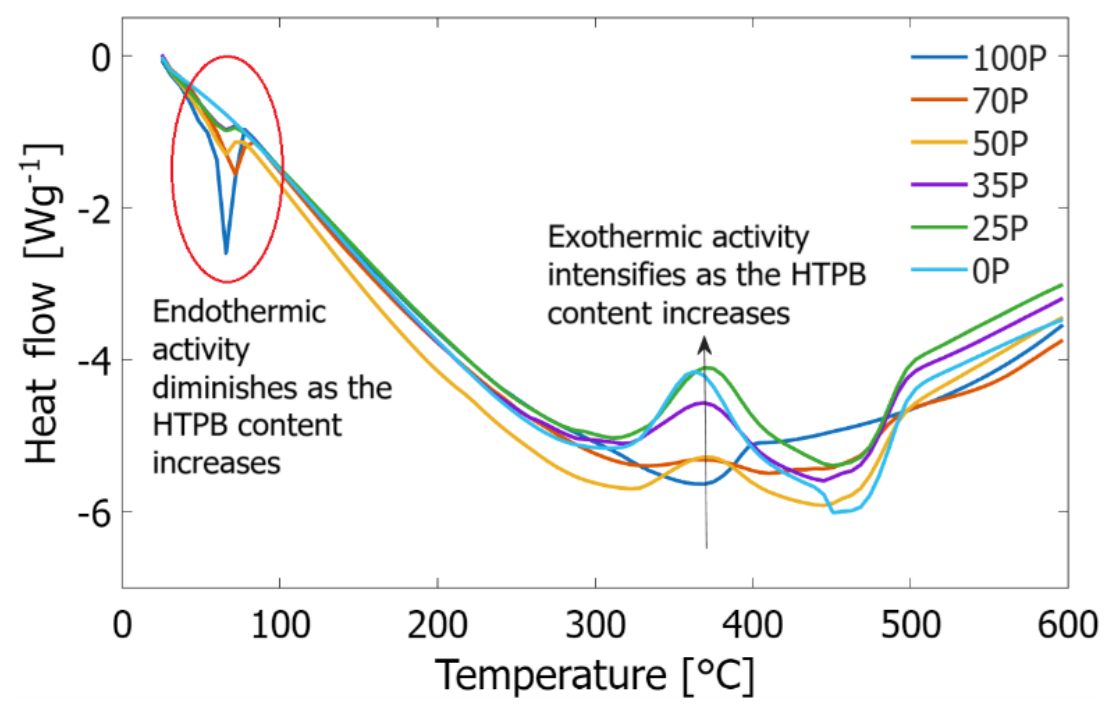


Fig 4. DSC curves showing the thermal transition behavior of paraffin, HTPB, and their blends

to samples with intermediate concentrations.

Composition	Onset Temperature [°C]
Composition	Oliset Telliperature [C]
100P	312.4 ± 7.1
70P	311.1 ± 1.9
50P	337.5 ± 2.8
35P	376.4 ± 4.6
25P	386.8 ± 1.5
0P	416.0 ± 2.5

Table 3. TGA results for paraffin/HTPB fuel samples at varying composition.

Table 4. DSC results for paraffin/HTPB fuel samples at varying composition.

Composition	Melting Temperature [°C]	Decomposition Temperature [°C]
100P	65.5 ± 0.1	402.1 ± 9.8
70P	69.1 ± 0.5	373.1 ± 3.5
50P	64.2 ± 0.8	377.6 ± 0.9
35P	64.3 ± 1.2	375.5 ± 0.4
25P	63.2 ± 0.4	375.9 ± 0.5
0P	NA	368.1 ± 2.3

3.3. Regression rate studies

Lab-scale ballistic tests were carried out to evaluate the regression rate performance of paraffin–HTPB fuels and their blends. These tests allow direct comparison with pure HTPB and paraffin grains, helping to quantify improvements in regression behavior, combustion efficiency, and structural integrity achieved through blending. Regression rates for all fuel formulations were calculated from the weight loss method using oxygen as the oxidizer, with the results summarized in Table 5.

All tests were performed at an average oxidizer mass flux ranging from 25.24 to 35.40 kg/m 2 ·s. For pure paraffin fuel, the regression rate was the highest, reaching 0.90 mm/s at a mass flux of 25.25 kg/m 2 ·s, with a final port diameter of 47.8 mm and a port area of 0.001188 m 2 .

In comparison, blended fuels displayed lower regression rates. The 25P blend achieved a regression rate of 0.40 mm/s at 30.24 kg/m²·s, with a final port diameter of 33.6 mm and a port area of 0.000794 m². The 35P blend showed a slightly lower regression rate of 0.30 mm/s at 30.52 kg/m²·s, corresponding to a final port diameter of 33.3 mm and a port area of 0.000786 m². The 50P blend exhibited similar performance, with a regression rate of 0.30 mm/s at 25.36 kg/m²·s, and a final port diameter of 33.4 mm with a port area of 0.000789 m². Likewise, the 70P blend recorded a regression rate of 0.30 mm/s at the highest mass flux of 35.40 kg/m²·s, with a final port diameter of 33.5 mm and a port area of 0.000791 m². Finally, the 0P formulation (pure HTPB) demonstrated a regression rate of 0.40 mm/s at 27.56 kg/m²·s, with a final port diameter of 33.8 mm and a port area of 0.000798 m².

These results, summarized in Table 5, reveal a general decreasing trend in regression rate with increasing oxidizer mass flux. Pure paraffin stands out with the highest regression rate at the lowest G_{ox} , while the blends cluster around lower regression rates despite differences in HTPB content. The 25P and 0P fuels achieved the highest regression rates among the blends (0.40 mm/s), while the 35P, 50P, and 70P blends maintained similar values at 0.30 mm/s. This highlights the trade-off introduced by the addition of HTPB. Although it reduces the regression rate relative to paraffin, it provides significant structural and mechanical advantages, resulting in a compromise between fuel performance and grain integrity.

Figure 5 shows the combustion chamber pressure and thrust profiles for the paraffin (100P), 25P, 35P,

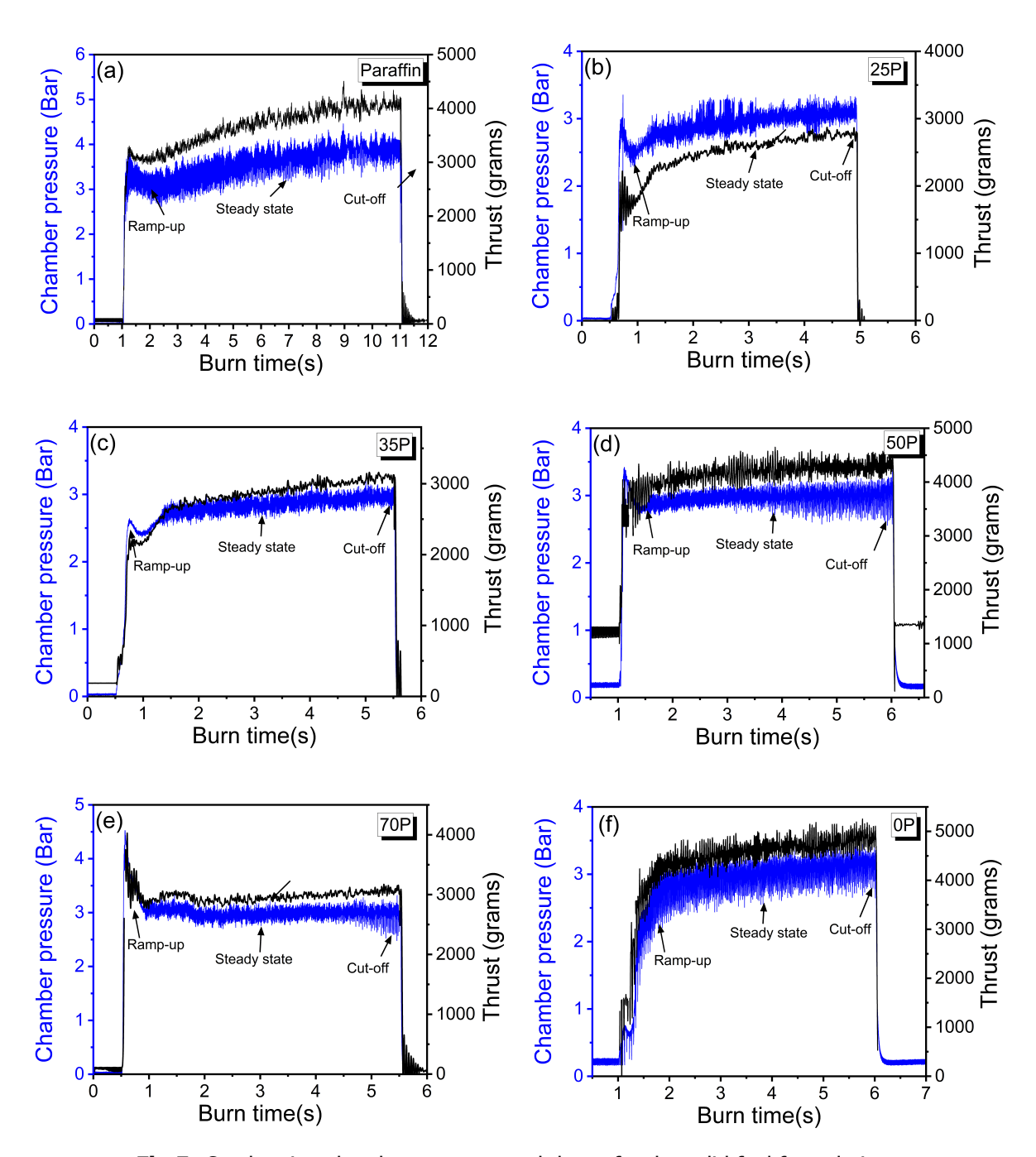


Fig 5. Combustion chamber pressure and thrust for the solid fuel formulations

50P, 70P, and 0P fuel formulations. The motor firing process can be divided into three main stages: ramp-up, steady state, and cut-off. Following ignition, a sharp pressure spike is observed due to the primer charge. The igniter then burns rapidly, releasing heat and combustion gases, which expand in the chamber and establish the ramp-up phase. Thrust rises noticeably after approximately 0.5 s as combustion stabilizes.

During steady-state operation, clear differences among the formulations are evident. The paraffin

Final Diameter	Regression Rate	Port Area	Oxidizer Mass Flux
d_f (mm)	\dot{r} (mm/s)	A_p (m^2)	G_{ox} (kg/(m $^2\cdot$ s))
47.8	0.9	0.001188	25.2485
33.6	0.4	0.000794	30.2429
33.3	0.3	0.000786	30.5155
33.4	0.3	0.000789	25.3554
33.5	0.3	0.000791	35.3953
33.8	0.4	0.000798	27.5621
	d_f (mm) 47.8 33.6 33.3 33.4 33.5	d_f (mm) \dot{r} (mm/s) 47.8 0.9 33.6 0.4 33.3 0.3 33.4 0.3 33.5 0.3	d_f (mm) \dot{r} (mm/s) A_p (m²) 47.8 0.9 0.001188 33.6 0.4 0.000794 33.3 0.3 0.000786 33.4 0.3 0.000789 33.5 0.3 0.000791

Table 5. Comparison of Parameters for Paraffin and HTPB blend

(100P) fuel achieved the highest performance, with chamber pressures reaching about 5.0 bar and thrust levels in the range of 3500-4000 q. In comparison, the 25P and 35P blends sustained chamber pressures near 3.0 bar, producing thrust levels of approximately 2500-3000 g and 2500 g, respectively, both showing a brief drop immediately after ignition before stabilization. The 50P blend exhibited intermediate behavior, maintaining pressures of 3 bar with thrust around 4000–4500 g, while the 70P blend showed a more stable but lower combustion performance with chamber pressure close to 3.0 bar and thrust in the range of 3000 g. Finally, the OP formulation (pure HTPB) demonstrated performance comparable to the 50P blend, sustaining chamber pressures around 3.5 bar and thrust levels of 5000 a.

Table 6. Steady-state chamber pressure and thrust for the different fuel formulations

Fuel	Chamber Pressure (bar)	Thrust (g)
Paraffin (100P)	~3.5	3500-4000
25P	∼3.0	2500–3000
35P	∼3.0	~3000
50P	∼3.0	4000–4500
70P	∼3.0	~3000
OP (HTPB)	∼3.0	4500–5000

In the final cut-off stage, all fuels exhibited a sharp and simultaneous pressure and thrust drop, corresponding to the termination of oxidizer supply and complete flameout.

4. Conclusions

The present study provides an experimental investigation of hydroxyl-terminated polybutadiene (HTPB), paraffin-based solid fuels, and their blends for hybrid rocket applications. Based on the results, the following conclusions can be drawn:

- Tensile tests indicate that HTPB-paraffin blends exhibit improved mechanical properties compared to pure paraffin, demonstrating sufficient structural integrity for potential hybrid rocket applications.
- Thermogravimetric analysis (TGA) shows that pure paraffin (100P) decomposes at $312.4 \pm$ 7.1 °C, while pure HTPB (0P) decomposes at 416.0 ± 2.5 °C. Blended fuels display intermediate decomposition temperatures, increasing with HTPB content, confirming that HTPB enhances thermal stability.
- Differential scanning calorimetry (DSC) reveals that paraffin-containing blends melt between 65.5 ± 0.1 °C (100P) and 63.2 ± 0.4 °C (25P), whereas pure HTPB shows no melting. Increasing HTPB content reduces melting activity while enhancing exothermic decomposition, balancing paraffin's melting behavior with HTPB's thermal stability.

• Ballistic testing demonstrates that pure paraffin exhibits the highest regression rate, while blends with increasing HTPB content show progressively lower regression rates, highlighting the trade-off between fuel regression and mechanical integrity.

5. Acknowledgements

The authors gratefully acknowledge the SIA Advanced Space Propulsion Laboratory at the School of Aerospace Engineering - Sapienza University of Rome for their support and experimental facilities.

References

- [1] Pal, Y., Palateerdham, S. K., Mahottamananda, S. N., Sivakumar, S., & Ingenito, A., "Combustion performance of hybrid rocket fuels loaded with MgB2 and carbon black additives," Propulsion and Power Research, 12(2), 212–226, 2022. doi:10.1016/j.jppr.2022.11.003
- [2] Pal, Y., Mahottamananda, S. N., S, S., Palateerdham, S. K., & Ingenito, A., "Thermal decomposition kinetics and combustion performance of paraffin-based fuel in the presence of CeO2 catalyst," FirePhysChem, 3(3), 217–226, 2022. doi:10.1016/j.fpc.2022.10.005
- [3] Chiaverini, M. J., Serin, N., Johnson, D. K., Lu, Y.-C., Kuo, K. K., & Risha, G. A., "Regression Rate Behavior of Hybrid Rocket Solid Fuels," Journal of Propulsion and Power, 16, 125–132, 2000. doi:10.2514/2.5541
- [4] Kim, S., Moon, H., Kim, J., & Cho, J., "Evaluation of Paraffin—Polyethylene Blends as Novel Solid Fuel for Hybrid Rockets," Journal of Propulsion and Power, 31, 1750—1760, 2015. doi:10.2514/1.B35565
- [5] Mazzetti, A., Merotto, L., & Pinarello, G., "Paraffin-based hybrid rocket engines applications: A review and a market perspective," Acta Astronautica, 126, 286–297, 2016. doi:10.1016/j.actaastro.2016.04.036
- [6] Karabeyoglu, M. A., Altman, D., & Cantwell, B. J., "Combustion of liquefying hybrid propellants: Part 1, General Theory," Journal of Propulsion and Power, 18(3), 610–620, 2002. doi:10.2514/2.5975
- [7] Tian, H., Lu, Y., Li, L., Chen, R., Niu, X., Zhang, Y., & Cai, G., "Experimental investigation on thermal behavior and regression rate characteristics of paraffin-polyethylene wax blends as hybrid rocket fuels," Acta Astronautica, 2025. doi:10.1016/j.actaastro.2025.07.056
- [8] Thomas, J. C., Paravan, C., Stahl, J. M., Tykol, A. J., Rodriguez, F. A., Galfetti, L., & Petersen, E. L., "Experimental evaluation of HTPB/paraffin fuel blends for hybrid rocket applications," Combustion and Flame, 229, 111386, 2021. doi:10.1016/j.combustflame.2021.02.032
- [9] Bisin, R., Verga, A., Bruschi, D., & Paravan, C., "Strategies for Paraffin-based Fuels Reinforcement: 3D Printing and Blending with Polymers," AIAA Propulsion and Energy 2020 Forum, 2021. doi:10.2514/6.2021-3502
- [10] Sinha, Y. K., Sridhar, B. T. N., & Kishnakumar, R., "Study of Thermo-Mechanical Properties of HTPB-Paraffin Solid Fuel," Arabian Journal for Science and Engineering, 41(11), 4683–4690, 2016. doi:10.1007/s13369-016-2230-3
- [11] Mahottamananda, S. N., Kadiresh, N. P., & Pal, Y., "Regression rate characterization of HTPB–Paraffin based solid fuels for hybrid rocket," Propellants, Explosives, Pyrotechnics, 45(11), 1755–1763, 2020. doi:10.1002/prep.202000051
- [12] Paravan, C., Hashish, A., & Santolini, V., "Test activities on hybrid rocket engines: Combustion analyses and Green Storable Oxidizers—A short review," Aerospace, 10(7), 572, 2023. doi:10.3390/aerospace10070572
- [13] Carmicino, C., & Sorge, A. R., "Role of injection in hybrid rockets regression rate behaviour," Journal of Propulsion and Power, 21(4), 606–612, 2005. doi:10.2514/1.9945